17. P. D. Jones, *Geophys. Res. Lett.* **21**, 1149 (1994).
18. T. R. Karl, R. W. Knight, J. R. Christy, *J. Climate* **7**, 1144 (1994).
19. K. E. Trenberth, J. R. Christy, J. W. Hurrell, *ibid.* **5**, 1405 (1992).
20. P. D. Jones and T. M. L. Wigley, *Nature* **344**, 711 (1990).
21. J. R. Christy, R. W. Spencer, R. T. McNider, *J. Climate*, in press.
22. A. H. Gordon, *Nature* **367**, 325 (1994).
23. W. F. Ruddiman and A. McIntyre, *Science* **212**, 617 (1981).
24. R. A. Bryson, *Trans. Am. Geophys. Union* **29**, 473 (1948).
25. W. D. Sellers, *Physical Climatology* (Univ. of Chicago Press, Chicago, 1965).
26. Portions of this research were supported by NSF grant SES 9121398.

8 November 1994; accepted 11 January 1995

Conformation of Macromolecules in the Gas Phase: Use of Matrix-Assisted Laser Desorption Methods in Ion Chromatography

Gert von Helden, Thomas Wyttenbach, Michael T. Bowers*

Conformational data for macromolecules in the gas phase have been obtained by the coupling of a matrix-assisted laser desorption ion source to an ion chromatograph. A series of polyethylene glycol (PEG) polymers "cationized" (converted to a cation) by sodium ions (Na^+PEG9 to Na^+PEG19) and a protonated neurotransmitter protein, bradykinin, were studied. Mobilities of Na^+PEG9 to Na^+PEG19 are reported. Detailed modeling of Na^+PEG9 with molecular mechanics methods indicates that the lowest energy structure has the Na^+ ion "solvated" by the polymer chain with seven oxygen atoms as nearest neighbors. The agreement between the model and experiment is within 1 percent for Na^+PEG9, Na^+PEG13, and Na^+PEG17, giving strong support to both the method and the deduced structures. Similar agreement was obtained in initial studies that modeled experimental data for arginine-protonated bradykinin.

Determination of the preferred conformations of large molecules traditionally has been restricted to the condensed phase, both as a means of inhibiting intramolecular motion and as a way of increasing the number density of the target molecule. For biomolecules such as proteins, the relation between conformation and activity has long been an active area of research, especially the relation between protein folding and genetic expression (*1*). With the advent of matrix-assisted laser desorption ionization (MALDI) (*2*) and electrospray ionization (ESI) (*3*), it has become routine to desorb molecules of nearly any size into the gas phase, where they can be examined by mass spectrometry (*4*). A primary focus of this work has been the determination of structural features of these molecules. For example, considerable progress has been made in determining amino acid sequences of proteins (*5*) and, as an adjunct to this work, the importance of metal ions as cationizing agents both for sequence studies and for investigations of their influence on peptide chemistry (*6*, *7*).

More recently, attention has turned to conformational studies of macromolecules. For example, ESI charge distributions of select, multiply charged ions can change with solution properties such as pH or solvent. These results were interpreted in terms of conformational changes in the biomolecules of interest (*8*). Another approach involves counting the labile peptide protons by isotopic exchange, because the extent of exchange is believed to correlate with the degree of folding of the protein (*9*). Finally, the different collision cross sections that different conformers might exhibit have been used to distinguish "larger" conformers from "smaller" conformers of multiply charged ions in triple quadrupole instruments (*10*).

Each of the above conformational studies used ESI and hence dealt with multiply charged ions rather than singly charged ions. In addition, although the conclusions about the existence of different conformations were usually unambiguous, none of the methods were designed to give any detailed structural information on the various conformers observed. In this report, we describe the use of MALDI in conjunction with our recently developed ion chromatography (IC) technique (*11*). When combined with molecular mechanics-dynamics methods, these data provide unambiguous structural information on singly charged cationized macromolecules in the gas phase.

We investigated the gas-phase structure of various polyethylene glycol (PEG) polymers in the range PEG9 to PEG19 (that is, from 9 to 19 $-(CH_2CH_2O)-$ monomer units). These are ideal systems for an initial study because they give a range of molecules whose connectivities are known and that change in a known way. Hence, the effect of chain length on conformation can be studied. A known series also provides a stringent test of the IC method as it must be able to reproduce and account for these changes without changing the molecular parameters used in modeling the system. Moreover, because PEG is cationized by Na^+ in our experiments, we can investigate the metal ion binding site (or sites) in a series of macromolecules of significant size. Finally, the distribution of PEG neutral species results in a distribution of the cationized polymers formed in the MALDI process, reducing the intensity of any one system by about an order of magnitude and providing a real test of the sensitivity of the method. The success of these experiments prompted application to biopolymers, and our initial work on the polypeptide bradykinin yielded parent ion signals an order of magnitude greater than for individual PEG systems, which made data acquisition much easier. These results, which will be discussed briefly here, will be published elsewhere (*12*).

Ions were made in a MALDI source built at the University of California at Santa Barbara, which is described elsewhere (*13*).

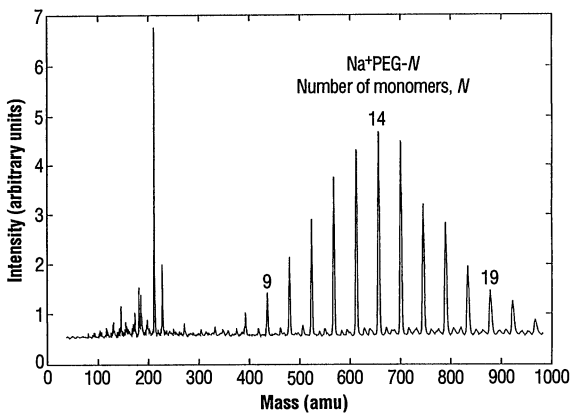

Fig. 1. A MALDI mass spectrum of a commercial PEG-600 sample present at 0.1% in a sinapinic acid matrix. All peaks below mass 300 (amu = atomic mass unit) are due to the matrix. A number of the Na^+-cationized PEG peaks are identified.

Department of Chemistry, University of California, Santa Barbara, CA 93106, USA.

*To whom correspondence should be addressed.

Briefly, the sample was deposited on a cylindrical drum that is attached to a screw thread. A synchronous motor slowly turned the screw such that a fresh area of sample on the drum was exposed for each laser shot. We used a Lambda Physik LPX-200 excimer laser running on N_2, yielding 10-ns pulses of ~1.5-mJ energy at 337 nm. For most studies, the sample was composed of a matrix of sinapinic acid and ~0.1% PEG-600. Ions emitted from the source were accelerated to 5 kV, mass-selected by a reverse–geometry sector mass spectrometer, decelerated to a few electron volts, and injected into the IC cell containing 5 torr of He at 300 K. The 10-ns laser pulse produced bursts of ions at the IC cell less than 10 μs in width, and no further gating was required. Arrival time distributions were obtained at the detector after passage through the quadrupole mass filter that follows the IC cell. Details of the instrument are given elsewhere (*14*).

A typical mass spectrum is shown in Fig. 1. A commercial sample of PEG-600 produced a series of peaks centered near a mass-to-charge ratio of 600 that corresponds to PEG species cationized by Na^+. Intensities were sufficient for IC studies of Na^+PEG9 to Na^+PEG19.

A typical arrival-time distribution (ion chromatagram) is given in Fig. 2 for Na^+PEG9. From distributions such as these, mobilities of the various Na^+-cationized PEG species can be obtained (*15*). The transport equations of an ion drifting through He gas under a uniform electric field can easily be solved (*16*), which yields the dashed line in Fig. 2 for an ion mobility of 4.2 $cm^2\ V^{-1}\ s^{-1}$; clearly, the agreement with experiment is excellent. The important point is that the IC peak can be fit essentially exactly with a single mobility. This fit excludes the existence of stable conformers that vary by more than 0.1 $cm^2\ V^{-1}\ s^{-1}$ from 4.2 $cm^2\ V^{-1}\ s^{-1}$ (that is, by more than 2.5%). These conformers would appear as obvious shoulders or as asymmetries in the experimental peak shape. Arrows in Fig. 2 are placed ±2.5% from the peak center, and no deviations from the expected peak shape were observed within these boundaries. However, the fit does not exclude rapidly interconverting isomers that yield an average mobility of 4.2 $cm^2\ V^{-1}\ s^{-1}$. Similar results were obtained for Na^+PEG10 to Na^+PEG19.

The question that now arises is: What is the structure of the conformer or set of conformers that gives rise to the IC spectra we obtain. We have discussed in detail the method we used to obtain such structures in our work on carbon clusters (*17*). In that work, we calculated a potential conformer structure by using either ab initio or semiempirical methods. The angle-averaged collision cross section of the conformer with He was then obtained with Monte Carlo methods. The mobility is simply inversely proportional to the cross section in the hard-sphere limit. If the mobility of the predicted structure was within 2% of the experimental value, then it became a candidate for the actual conformer structure. Usually, the agreement was within 1% for successful candidates.

The Na^+PEG systems considered here are too large for either ab initio or semiempirical methods, so instead we performed molecular mechanics calculations with the force field found in the Sybyl set of programs (*18*). We began with Na^+PEG9 and used the random selection aspect of the program to generate 400 stable conformers. Their relative energies varied over a range of ~60 kcal mol^{-1}, and the associated mobilities from ~4.3 to ~2.5 $cm^2\ V^{-1}\ s^{-1}$. Examination of the structures of the lowest energy conformers showed that all of them had multiple O atoms coordinated about the Na^+ center. A series of annealings and energy minimizations (*13*) generated the lowest energy structure. This structure is shown in Fig. 3 for Na^+PEG9. In order to best compare with experiment, we performed a 300 K molecular dynamics simulation on this 0 K structure for 200,000 fs. We calculated mobilities by sampling the instantaneous structure at 100-fs intervals (2000 mobility calculations in all), yielding a value of K_o = 4.20 ± 0.10 $cm^2\ V^{-1}\ s^{-1}$. The uncertainty given is the maximum spread obtained in the simulation. This value agrees very well with the experimental value of K_o = 4.18 ± 0.05 $cm^2\ V^{-1}\ s^{-1}$. No adjustable parameters were used to obtain a fit of the model to the experiment (*19–21*).

The structure shown in Fig. 3 is a stick-and-ball structure with artificial atom sizes selected to highlight the location of the Na^+ ion and the O atoms. The H atoms are excluded (for clarity). The PEG9 structure coils around the Na^+ ion such that five O atoms are nearest neighbors in a plane, and single additional O atoms both above and below the plane give a total of seven O nearest neighbors. Each O atom is ~2.2 Å from the Na^+ ion. A space-filling model in

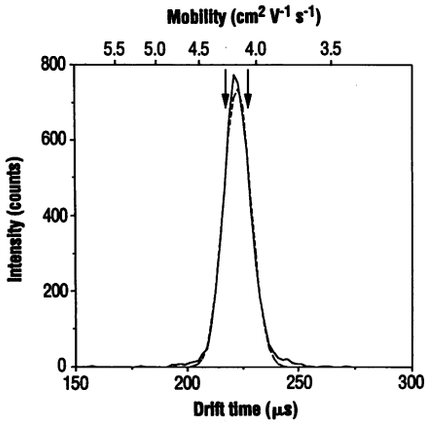

Fig. 2. An arrival time distribution (ion chromatagram) for Na^+PEG9. The solid line is the experimental result, and the dashed line is a fit obtained by solving the transport equations for a single species with a mobility of 4.2 $cm^2\ V^{-1}\ s^{-1}$. The two arrows indicate a shift in the peak center of ±2.5% (see text).

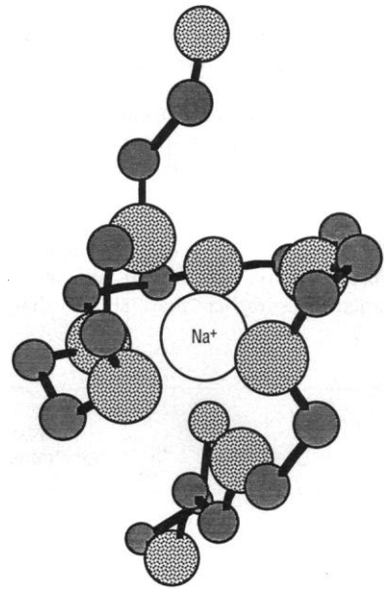

Fig. 3. A ball-and-stick structural representation of the lowest energy conformer of Na^+PEG9. The O atoms are shown as the larger speckled circles and the C atoms as the small, darker circles. The H atoms are not shown (for clarity). The sizes of the various atoms were chosen to highlight the interaction of Na^+ with the O atoms.

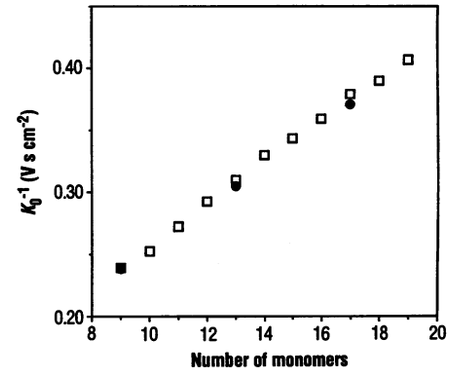

Fig. 4. A plot of K_o^{-1} versus number of monomers for the cationized PEG species Na^+PEG9 through Na^+PEG19. The open squares are the experimental data. The filled circles are the model-generated mobilities for Na^+PEG9, Na^+PEG13, and Na^+PEG17. The sizes of the points were chosen to include the uncertainties in the numbers.

which the van der Waals radii of the atoms are used indicates that the Na^+ ion is completely encased by the coiled PEG9.

The experimental data for other systems are given in Fig. 4 as a plot of K_o^{-1} versus the number of monomers. A regular, near-linear increase with monomer number is observed as expected for members of a single structural family (*17*). We have modeled Na^+PEG13 and Na^+PEG17 in addition to Na^+PEG9, and these three data points are shown in Fig. 4 for comparison. Excellent agreement was obtained between the model and experiment. Modeling of the complete series will be reported elsewhere (*13*).

The Sybyl molecular mechanics programs were also used to model the possible stable conformers of the neutral PEG9. A series of 400 stable conformers were randomly generated with resulting relative energies over a range of ~20 kcal mol^{-1}. Several of the more stable species were annealed and subjected to energy minimization. The most stable of these was then subjected to 200,000 fs of molecular dynamics at 300 K, and 2000 structures were extracted at 100-fs intervals. The mobilities these species would have generated if singly charged were in the range $K_o = 3.5 \pm 0.4$ cm^2 V^{-1} s^{-1}. This lower value of K_o indicates that a much more open structure is predicted for neutral PEG9 relative to Na^+PEG9, and the molecular dynamics simulation reveals that a much wider range of conformers is sampled at 300 K. Both results are consistent with rather weak intramolecular interactions in neutral PEG9 relative to Na^+PEG9.

A few words of comparison with our bradykinin results (*12*) are useful. Bradykinin is almost exclusively cationized with protons, rather than with Na^+ in our experiments, regardless of the matrix. Protons prefer to form localized bonds, and, if the charge is shared, they usually involve only two centers. Furthermore, bradykinin has two arginine units, one at the NH_2-terminus and one at the COOH-terminus, which are preferred sites of protonation (*22*). Hence, one might expect a more open structure for protonated bradykinin (a nine-residue peptide chain) than for Na^+-cationized PEG structures. Our modeling suggests that this is the case. The experimental mobility is 2.20 ± 0.05 cm^2 V^{-1} s^{-1}, and our preliminary modeling results, assuming protonation at arginine, yield a mobility of ~2.1 cm^2 V^{-1} s^{-1} for the lowest energy structure. The model result needs to be subjected to molecular dynamics averaging, and searches for other possible protonation sites need to be done. Nonetheless, the agreement is remarkably good and lends strong support both for the Sybyl molecular mechanics force field (*18*) and for our method for determining the van der Waals radii of the involved atoms (*19–21*).

REFERENCES AND NOTES

1. F. M. Richards, *Sci. Am.* **264**, 54 (January 1991).
2. M. Karas and F. Hillenkamp, *Anal. Chem.* **60**, 2299 (1988); R. C. Beavis and B. T. Chait, *Rapid Commun. Mass Spectrom.* **3**, 432 (1989); *ibid.*, p. 436.
3. C. M. Whitehouse, R. N. Dreyer, M. Yamashuta, J. B. Fenn, *Anal. Chem.* **57**, 675 (1985); J. B. Fenn, M. Mann, C. K. Meng, S. F. Wong, C. M. Whitehouse, *Science* **264**, 64 (1989).
4. See the special issue on mass spectrometry, *Acc. Chem. Res.* **27**, issue 11 (November 1994).
5. See, for example, B. T. Chait, R. Wang, R. C. Beavis, S. B. H. Kent, *Science* **262**, 89 (1993); K. Biemann, *Fresenius Z. Anal. Chem.* **343**, N1:25 (1992); *Annu. Rev. Biochem.* **61**, 977 (1992).
6. For leading references on alkali metals and peptides, see: R. B. Cody, J. I. Amster, F. W. McLafferty, *Proc. Natl. Acad. Sci. U.S.A.* **82**, 6367 (1985); L. M. Mallis and D. H. Russell, *Anal. Chem.* **58**, 1076 (1986); X. Tang, W. Eus, K. G. Standing, J. B. Westmore, *ibid.* **60**, 1791 (1988); R. P. Grese, R. L. Cerny, M. L. Gross, *J. Am. Chem. Soc.* **111**, 2835 (1989); J. A. Leary, T. D. Williams, G. Bott, *Rapid Commun. Mass Spectrom.* **3**, 192 (1989); L. M. Teesch and J. Adams, *J. Am. Chem. Soc.* **113**, 812 (1991).
7. For leading references on alkaline earth and transition metal ions, see: L. M. Teesch and J. Adams, *J. Am. Chem. Soc.* **112**, 4110 (1990); P. Hu and M. L. Gross, *ibid.* **114**, 9153 (1992); H. Zhoo, A. Reiter, L. M. Teesch, J. Adams, *ibid.* **115**, 2854 (1993); P. Hu and M. L. Gross, *ibid.*, p. 8821.
8. S. K. Chowdhung, V. Katta, B. T. Chait, *ibid.* **112**, 9012 (1990); J. A. Loo, R. R. Ogorzalek-Loo, H. R. Udseth, C. G. Edmunds, R. D. Smith, *Rapid Commun. Mass Spectrom.* **5**, 101 (1991); R. Gueuremont, K. W. M. Sui, J. C. Y. LeBlanc, S. S. Berman, *J. Am. Soc. Mass Spectrom.* **3**, 216 (1992).
9. V. Katta and B. T. Chait, *Rapid Commun. Mass Spectrom.* **5**, 214 (1991); B. E. Winger, K. J. Light-Wahl, A. L. Rockwood, R. D. Smith, *J. Am. Chem. Soc.* **114**, 5897 (1992); D. Suekau *et al.*, *Proc. Natl. Acad. Sci. U.S.A.* **90**, 790 (1993).
10. T. Covey and D. J. Douglas, *J. Am. Soc. Mass Spectrom.* **4**, 616 (1993); K. A. Cox, R. K. Julian, R. G. Cooks, R. E. Kaiser, *ibid.* **5**, 127 (1994).
11. M. T. Bowers, P. R. Kemper, G. von Helden, P. A. M. van Koppen, *Science* **260**, 1446 (1993).
12. T. Wyttenbach, G. von Helden, M. T. Bowers, unpublished results.
13. G. von Helden, T. Wyttenbach, M. T. Bowers, *Int. J. Mass Spectrom. Ion Processes* (Al Nier special issue), in press.
14. P. R. Kemper and M. T. Bowers, *J. Am. Soc. Mass Spectrom.* **1**, 197 (1990).
15. ———, *J. Phys. Chem.* **95**, 5134 (1991).
16. E. A. Mason and E. W. McDaniel, *Transport Properties of Ions in Gases* (Wiley, New York, 1988).
17. G. von Helden, M.-T. Hsu, N. Gotts, M. T. Bowers, *J. Phys. Chem.* **97**, 8182 (1993).
18. M. Clark, R. D. Cramer III, N. van Opdenbosch, *J. Comput. Chem.* **10**, 982 (1989).
19. The van der Waals radii used were 1.09 Å for He, 1.51 Å for O, 1.10 Å for H, and 1.61 Å for C. The He and C van der Waals radii were the same as those used for very extensive C studies (*17*). The H and O radii were determined by He scattering calculations on CH_4 and $(C_2H_5)_2O$, respectively. More details are given in (*20*) and (*21*).
20. G. von Helden, E. Porter, N. G. Gotts, M. T. Bowers, *J. Phys. Chem.* (Mostafa El Sayed special issue), in press.
21. G. von Helden, thesis, University of California at Santa Barbara (1994).
22. G. S. Gorman, J. P. Speir, C. A. Turner, I. J. Amster, *J. Am. Chem. Soc.* **114**, 3986 (1992).

23. This work was supported under NSF grants CHE91-10752 and CHE94-21176 and by the Air Force Office of Scientific Research under grant FA 9620-93-1-0134.

13 October 1994; accepted 10 January 1995

Control of IκB-α Proteolysis by Site-Specific, Signal-Induced Phosphorylation

Keith Brown, Susan Gerstberger, Louise Carlson, Guido Franzoso, Ulrich Siebenlist*

IκB-α inhibits transcription factor NF-κB by retaining it in the cytoplasm. Various stimuli, typically those associated with stress or pathogens, rapidly inactivate IκB-α. This liberates NF-κB to translocate to the nucleus and initiate transcription of genes important for the defense of the organism. Activation of NF-κB correlates with phosphorylation of IκB-α and requires the proteolysis of this inhibitor. When either serine-32 or serine-36 of IκB-α was mutated, the protein did not undergo signal-induced phosphorylation or degradation, and NF-κB could not be activated. These results suggest that phosphorylation at one or both of these residues is critical for activation of NF-κB.

Proteolytic degradation of IκB-α is essential for activation of NF-κB (*1–4*). When degradation is blocked by certain protease inhibitors that target proteasomes, activation of NF-κB is prevented. Physiologic stimulation also induces phosphorylation of IκB-α (*1–7*), but the significance of this phosphorylation for activation of NF-κB in cells has remained unclear. Induced phosphorylation does not in itself dissociate complexes of IκB-α and NF-κB in vivo (*1, 2, 4, 7*). The question arises as to how proteolysis of IκB-α is triggered.

To identify regions in IκB-α essential for signaling and degradation, we systematically mutated the human IκB-α gene and stably transfected the altered genes into mouse EL-4 T lymphocytes (*8–10*). Human IκB-α was distinguished from endogenous murine IκB-α by its slower mobility on SDS gels. The exogenous human wild-type IκB-α and endogenous murine IκB-α were degraded with similar kinetics upon cellular stimula-

Laboratory of Immunoregulation, National Institute of Allergy and Infectious Diseases, National Institutes of Health, Building 10, Room 11B16, Bethesda, MD 20892–1876, USA.

*To whom correspondence should be addressed.